Proceedings of the 10th World Congress on Civil, Structural, and Environmental Engineering (CSEE 2025)
Barcelona, Spain - April, 2025
Paper No. ICGRE 172
DOI: 10.11159/icgre25.172

Numerical Failure Analysis of Cut and Cover Tunnel Against Surface Blast

Abdullah H Alsabhan[1], Mohammad Asim Ansari [2], Ibraheem Rais[2], Md Rehan Sadique[2], Shamshad Alam[1], Wagdi Hamid[1]

[1]Department of Civil Engineering, College of Engineering, King Saud University
Riyadh-11421, Saudi Arabia
aalsabhan@ksu.edu.sa; salam@ksu.edu.sa; whamid@ksu.edu.sa

[2]Department of Civil Engineering, Zakir Hussain College of Engineering & Technology, Aligarh Muslim University
Aligarh, 202002, India
civilasimansari@gmail.com; ibraheemrais2336@gmail.com; rehan.sadique@zhcet.ac.in

Abstract **-** The cut-and-cover approach is widely utilized in the construction of shallow utility and transportation tunnels among many tunneling methods. Metro cities and their suburbs globally feature both bottom-up and top-down cut-and-cover tunnels. This work employs numerical analysis to evaluate a cut-and-cover tunnel situated beneath an active roadway in response to accidental surface blast loads, utilizing the finite element approach. The adjacent soil has been represented using the Mohr-Coulomb Plasticity (MC) model. The Concrete Damage Plasticity (CDP) model accounts for concrete behavior, whereas the Johnson-Cook (JC) model represents the elasto-plastic behavior of steel reinforcement. The US Army's CONWEP (Conventional Weapons) model integrates the explosion effects of trinitrotoluene (TNT) explosive material on the soil tunnel model. This numerical analysis was performed on sandy clay soil, with the TNT weight deemed similar to that of a small delivery truck's capacity i.e. (1814 kg). The soil cover above the underground structure has been adjusted based on the d/H ratio (where d represents the depth of the soil cover and H denotes the height of the tunnel cross-section). Ultimately, a mitigation analysis has been conducted by substituting the concrete with an energy-absorbing material, steel-fiber-reinforced concrete (SFRC), for the tunnel liner. SFRC substantially mitigates tensile damage in the concrete liner, hence improving tunnel safety.

Keywords**:** Vehicle blast; Finite element method; Numerical Modelling; Cut and cover tunnel

1. Introduction

Cut and cover tunnels are a common type of underground construction used for building transportation systems, underground parking lots, and other underground structures. These tunnels are created by excavating a trench, constructing a roof over it, and then filling the trench back in. The construction of cut and cover tunnels requires a significant amount of planning, engineering, and safety measures, particularly when considering potential risks from surface blasts.

Numerical studies conducted by researchers have been observed in the available literature. Wang et al. [1] conducted a numerical study in hydrodynamic software AUTODYN-2D to study the stress-wave propagation in three-phase soil. The numerical results also indicate that the attenuations of the peak particle velocity and peak pressure follow two linear curves. At a short distance from the explosion center, all three phases in the soil deform simultaneously. Feldgun et al. [2] investigated a numerical simulation of the internal blast of a buried tunnel with a liner and explosive considered in a steel cylindrical pipeline. Tiwari et al. [3] investigated an underground 3D circular tunnel against internal blast using finite element software Abaqus/Explicit. They observed that deformation in the tunnel liner increased with increasing explosive weight and decreased with the thickness of the tunnel liner. Varma et al. [4] performed a numerical analysis against seismic loading conditions in jointed rocks and concluded that shallow tunnels are more susceptible to seismic loading against damage analysis. Goel et al. [5] conducted a numerical study in Abaqus/Explicit finite element software in unsaturated and saturated soils for arched, circular, and rectangular cross sections of the tunnel and observed that the tunnel in saturated soil experienced less settlement as compared to the tunnel considered in unsaturated soil. Lower tensile damage was observed in the tunnel with a circular shape as compared to other shapes under consideration. Propagation waves reached the surface earlier in cases of saturated soil. Sadique et al. [6] analyzed a numerical study to understand the behavior of three rocks, namely quartzite,

granite, and basalt, while maintaining the constant geometry of the model. Quartzite is more resistant to rocks, and granite is the least resistant against blast loading. Senthil et al. [7] conducted a numerical study in Abaqus and concluded that square-shaped tunnel cross sections are more vulnerable to blasts than the circular-shaped tunnel cross section.

Based on the available literature, it can be inferred that the majority of assessments of surface or subsurface blasts were conducted on subterranean constructions such as tunnels. However, no research has examined the behavior of cut and cover tunnels subjected to surface blasts due to vehicle explosions containing TNT. Abaqus/Explicit [8], has been used for finite element analysis. Additionally, to further increase tunnel stability, consider strengthening the concrete and mitigating its effects with a metallic liner (SFRC).

2. Constitutive Material Modelling

In the present study, to analyze the effect of the explosion of the vehicle against the tunnel, different material models have been adopted to incorporate their behavior. This section discusses the introduction of the Mohr-Coulomb (M-C) model in order to account for the plastic behavior of soil, the Concrete Damage Plasticity (CDP) model to account for the inelastic behavior of concrete, which includes both compressive and tensile behavior, the Johnson-Cook (J-C) model to account for the elastic and plastic behavior of steel reinforcement bars, which takes into account the effects of temperature, strain rate, and stress state, the CONWEP model to incorporate the explosive trinitrotoluene (TNT), and the behavior of SFRC too has been incorporated according to the CDP model.

2.1. Mohr-Coulomb Plasticity Model for Soil

A Mohr-Coulomb plasticity model was used in this study to simulate soil behavior, incorporating both isotropic hardening and softening characteristics. . The yield function as per the M-C plasticity failure criterion is given by the equation (1).

$$\tau = c + \sigma \tan\phi \tag{1}$$

Where τ is the shear stress, c is the cohesion of the soil, σ is the normal stress acting on the plane, and ϕ is the angle of internal friction of the soil.

A model to represent the general stress invariants can be written as:

$$F = R_{mc} q - p\tan\phi - c = 0 \tag{2}$$

Where,

$$R_{mc}(\theta,\phi) = \frac{1}{\sqrt{3}\cos\phi}\sin\left(\theta + \frac{\pi}{3}\right) + \frac{1}{3}\cos\left(\theta + \frac{\pi}{3}\right)\tan\phi \tag{3}$$

$$\cos(3\theta) = \left(\frac{r}{q}\right)^3 \tag{4}$$

$$p = -\frac{1}{3}trace(\sigma) \tag{5}$$

$$q = \sqrt{\frac{1}{3}(S:S)} \tag{6}$$

$$r = \left(\frac{9}{2}S * S:S\right)^{\frac{1}{3}} \tag{7}$$

$$S = \sigma + pI \tag{8}$$

where θ (deviatoric polar angle), p (equivalent pressure stress), q (Mises equivalent stress), r (third invariant of deviatoric stress), and S (deviatoric stress) are the different parameters, and Table 1 and Table 2 present the properties of sandy clay soil and its hardening properties, respectively [9].

Table 1: Mechanical properties of soil [9]

Unit Weight (kN/m³)	Cohesion (kN/m²)	Angle of friction (°)	Modulus of Elasticity (MPa)
17.71	92	23	16.8

Table 2: Hardening Properties [9]

Cohesion yield stress (Pa)	Absolute plastic strain
92000	0
21000	0.015

330000	0.065
360000	0.12

2.2. CDP model for Concrete

Tunnel liner material concrete with grade M30 has been used in this study. The concrete damaged plasticity model (CDP), which offers a comprehensive capacity for modeling concrete and other quasi-brittle materials, has been employed in finite element modeling to characterize the inelastic behavior of concrete [10]. According to the model, the concrete material fails mostly due to tensile cracking and compressive crushing.

The input parameter of M30 grade concrete is shown in Table 3 [11]. The tensile behaviour of concrete and the compressive behaviour of the concrete has been considered from literature [10].

Table 3: Input Parameter of M30 grade Concrete [11]

Grade of concrete	Mass density (kg/m^3)	Young's modulus (GPa)	Poisson's ratio	Dilation angle (˚)	Eccentricity	fb_0/fc_0	k	Viscosity parameter
M30	2500	26.6	0.2	31	0.1	1.16	0.67	0

2.3. Johnson-Cook's model for Reinforcement

The elasto-viscoplastic material model by Johnson and Cook [12] has been employed to forecast the flow and fracture characteristics of reinforcement. The von Mises yield criterion and its associated flow rule constitutes the basis for the material model. This model accounts for the non-linearity of the steel reinforcement (Grade Fe415 according to IS:456 2000 code of practice), with properties detailed in Table 4 [13]. The stress-strain connection in the reinforcement can be expressed as illustrated.

$$\sigma = \left(A + B\epsilon^{n}\right)\left(1 + Cln\varepsilon^{*}\right)\left(1 - T^{*m}\right) \tag{9}$$

Where, ε^{*} stands for plastic strain, A, B, C and m, n are model parameters and T^{*} represent the homologous temperature.

Table 4: Input Properties of steel reinforcement [13]

Density (Kg/m3)	Modulus of Elasticity (GPa), E	Poisons ratio, ν	Static yield strength, A (Mpa)	Strain hardening constant, B (Mpa)	Thermal softening exponent, m	Strain hardening exponent, n
7850	210	0.3	490	807	0.94	0.73

2.4. CONWEP model for explosive

The Conventional Weapons (CONWEP) model has been used in the current study to simulate the explosive (TNT), and the simulation has been run for 0.35 seconds. The 1814 kg TNT explosive utilized in this study is transported in a small delivery truck [14]. The US Army handbook TM5-855-1, "Design and Analysis of Hardened Structures to Conventional Weapons Effects," which contains experimental data and the blast loading equations put out by Kingery and Bulmash [15], serves as the foundation for the CONWEP function. This model utilizes the user-defined equivalent TNT explosive weight to calculate the necessary blast pressure. The pressure generated during the blast can be determined as follows:

$$cos\theta \geq 0$$
$$p(t) = P_{incident}(t)\left[1 + cos\theta - 2cos^{2}\theta\right] + P_{reflected}(t)cos^{2}\theta \tag{10}$$
$$cos\theta \leq 0$$
$$p(t) = P_{incident} \tag{11}$$

where, incident pressure ($P_{incident}$), reflected pressure ($P_{reflected}$) and angle of incidence is θ.

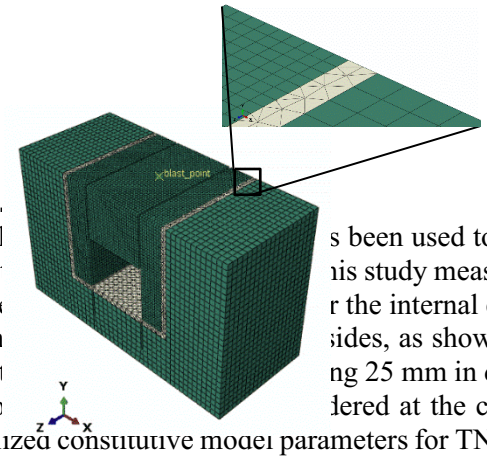

3.

Tl s been used to create the models for the soil, concrete, reinforcement, and explosive. The soil model ıis study measured (46 m x 28.2 m x 20 m) as shown in figure 1a. The dimensions of the tunnel have b r the internal clear cross section, with a side wall thickness of 1 m and a 1.2 m top and bottom slab an ;ides, as shown in figure 1b [16]. Figure 1c illustrates the two layers of reinforcement in the concre ng 25 mm in diameter along the length and 20 mm in diameter in the transverse direction. The point c dered at the center of the top surface of the model. The literature provides both general and specialized constitutive model parameters for TNT; however, ABAQUS/Explicit uses the default TNT values from the CONWEP model to simulate the blast.

The finite element tool's contact algorithm has defined the surface-to-surface contact between the surrounding soil and the tunnel lining, as well as a tangential interaction. The entire concept of the soil-tunnel has been opted, with the tunnel as the master and the soil's contact surface as the slave surface. The FE mesh that is accessible in FEM uses C3D8R (eight-node brick element with reduced integration, hourglass control, and finite membrane strains). The soil has been meshed with C3D8R elements and C3D4 (a 4-node linear tetrahedron) elements with a modified formulation having linear bulk viscosity factor unity. The C3D8R elements can simulate the blast reaction of the structure. The reinforcement bars have been modeled using B31 (two-node beam elements) [3]. Figure 2 shows the meshing of the soil and liner. For adopting the size of the elements, meshing studies have been performed from the smallest size, 100 mm, to the largest size, 1200 mm. As shown in Figure 3, the graph tends to stabilize after 400 mm. However, to reduce the simulation time and to minimize system space utilization. It has been decided to take 500 mm of elemental soil for the specific region under concern, and 250 mm has been taken for the concrete liner. Boundary conditions of the model have been defined, i.e., $U_x = U_y = U_z = U_{rx} = Ury = U_{rz} = 0$ (bottom fixed), $U_x = U_{ry} = U_{rz} = 0$ (both sides in x-direction side roller support), and $U_z = U_{rx} = U_{ry} = 0$ (front and back side roller support). The total number of elements is 117,526, out of which 87,308 are C3D8R types, 15,928 are C3D4 types, and 14,920 are beam elements.

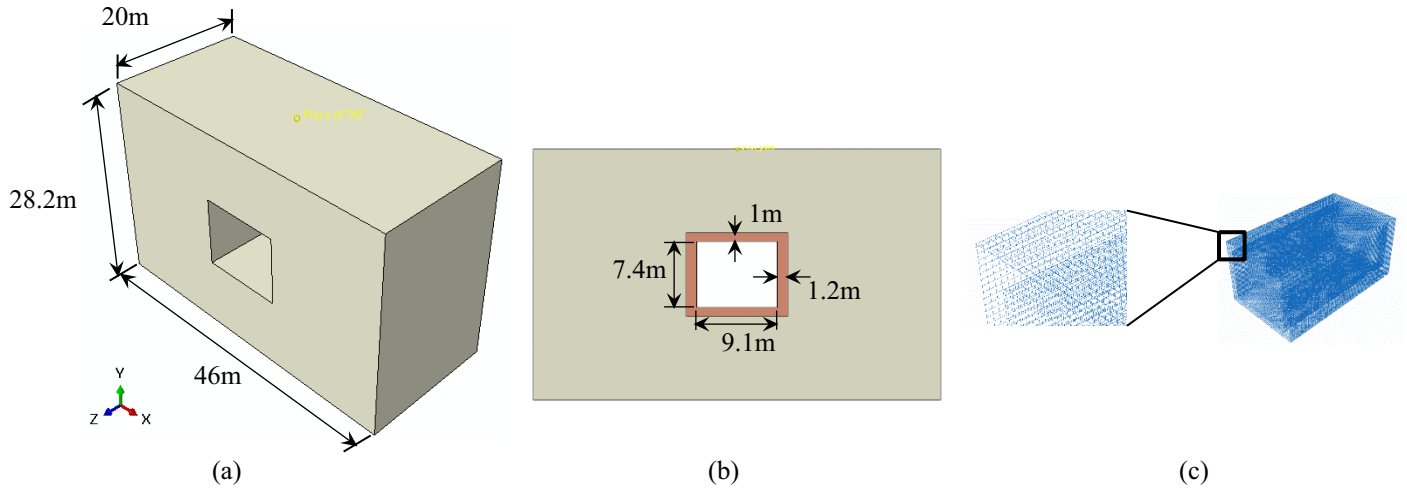

Fig. 1: Details of Geometry of Model (a) Soil Model (b) Concrete Tunnel liner model (c) Reinforcement for liner model

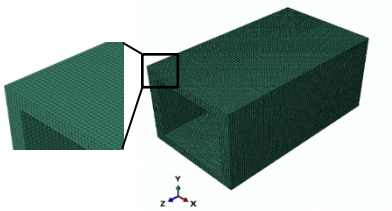

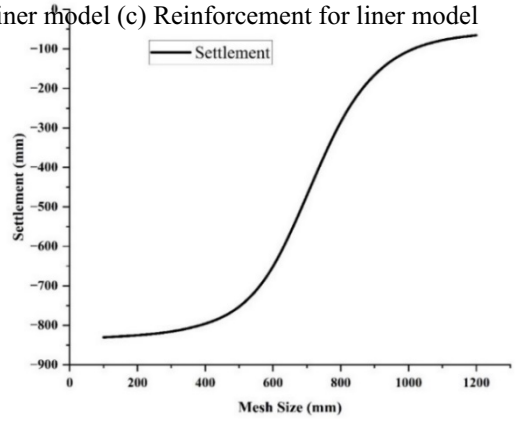

(a) (b)

Fig. 2: Meshing of (a) Soil model (b) Concrete tunnel lining model

Fig. 3: Mesh convergence of soil study

4. Validation by Empirical Relation

Upon detonation of a surface explosive, the ground is compressed and compacted, resulting in the formation of a crater as the blast wave interacts with the surface. The mass of the charge and soil properties like as void ratio, density, compressive strength, and mineral composition influence the dimensions of the crater. A Finite Element soil model without a tunnel liner has been created with a mesh size of 0.8m to validate the numerical research for the crater. The dimensions of models created by Soil are 46m x 28.2m x 20m. For validation, five explosive charges with weights of 50, 100, 150, 200, and 250 kg were evaluated. We analyzed the radius of the craters generated by five distinct explosive charges on the soil's surface. The crater radius determined by using the equation 12 from Ambrosini et al. [17] is compared with the crater radius derived from the numerical analysis of five TNT charges. The mean percentage variance is just 7.12. Figure 4 illustrates the comparison between numerical and empirical crater sizes.

$$D = 0.51\ W_3^{\frac{1}{3}} \tag{12}$$

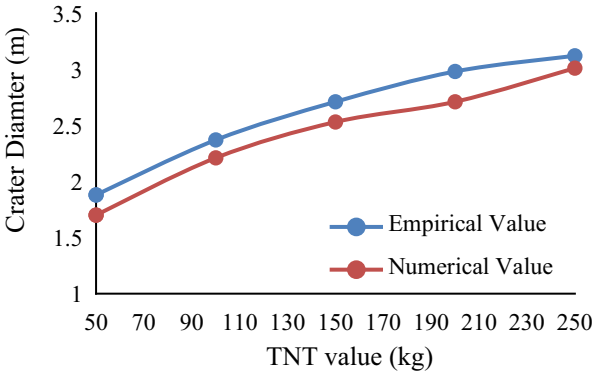

Fig. 4: Comparison of empirical and numerical crater diameter

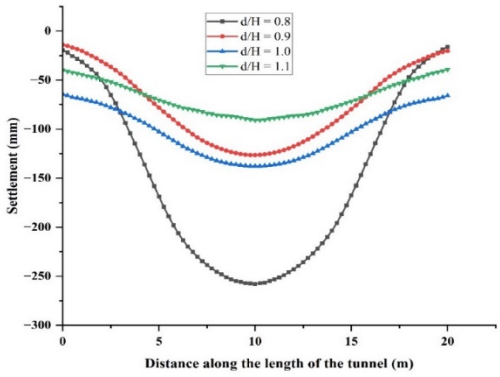

Fig. 5: Settlement variation in the top slab of the concrete tunnel liner

5. Results and Discussion

The present study has been conducted in sandy clay under the explosion of a 1814kg TNT (Small delivery truck capacity). It used different material models, such as the M-C plasticity model for soil modeling, the CDP model for concrete modeling, and the J-C model for reinforcement modeling. It has observed the tunnel's response to stresses, the settling of the concrete liner, and damage analysis. It has also reported this response under the variation of overburden depth (d/H = 0.8, 0.9, 1.0, 1.1). Finally, we conducted a mitigation study to minimize the explosion's effects. It conducted mitigation using an energy-absorbing material.

5.1. Effect of Cover Depth

The analysis has taken into account five scenarios (d/H = 0.8, 0.9, 1.0, and 1.1) to examine the impact of the cover thickness above the underground structure, all while maintaining a constant height of the tunnel cross section. The detonation point is at the top of the surface of the model, which means a blast is an external explosion. By varying the soil cover over the cut and cover tunnel, this parametric study aims to protect the underground structure from surface blasts caused by the explosion of 1814 kg TNT.

This parametric study has observed settlements in the top slab along a path equal to the tunnel's length. It reports a maximum settlement value of 257.88 mm for the ratio d/H = 0.8, which decreases as the soil cover increases over the tunnel and 90.83 mm

for the ratio d/H = 1.1. One of the reasons behind the reduction in the settlement value from the ratio d/H=0.8 to d/H=1.1 can be stated as the increase in the cover thickness. The percentage of increasing resistance from the ratio 0.8 to 1.0 is 46.85%; however, from 1.0 to 1.1 is 33.73%. The graphs show the variation in settlement in the top slab of the tunnel liner in Figure 5. Figure 6 displays the settlement contours in the negative y-direction.

In this parametric study, Figure 7 illustrates the mises stresses in the tunnel liner against the container blast. The case with the least soil cover showed the highest mises stress, which decreased up to a ratio of d/H = 1.0. After that, it observed an increase in the stress value, potentially due to an increase in the soil's dead load. Researchers have reported maximum stress values of 22.28 MPa, 20.88 MPa, 18.84 MPa, and 21.26 MPa for ratios of 0.8, 0.9, 1.0, and 1.1, respectively.

Additionally, this parametric study conducted an analysis of the tensile damage in the concrete tunnel liner. The tensile damage value varied from 0 to 1, where 0 indicates no damage and 1 indicates complete damage to the structure. It observed the complete failure of the cut and cover tunnel in the case of the lowest soil cover and found that the destruction level decreased with increasing cover depth, as shown in Figure 8. The results displayed are after the removal of the damaged elements.

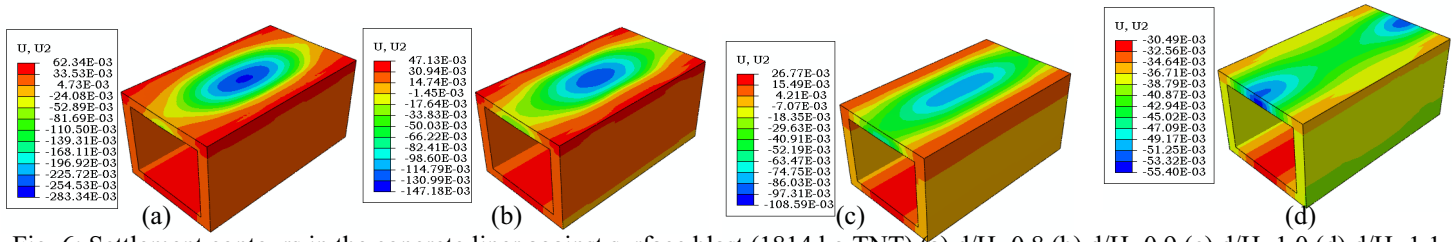

Fig. 6: Settlement contours in the concrete liner against surface blast (1814 kg TNT) (a) d/H=0.8 (b) d/H=0.9 (c) d/H=1.0 (d) d/H=1.1

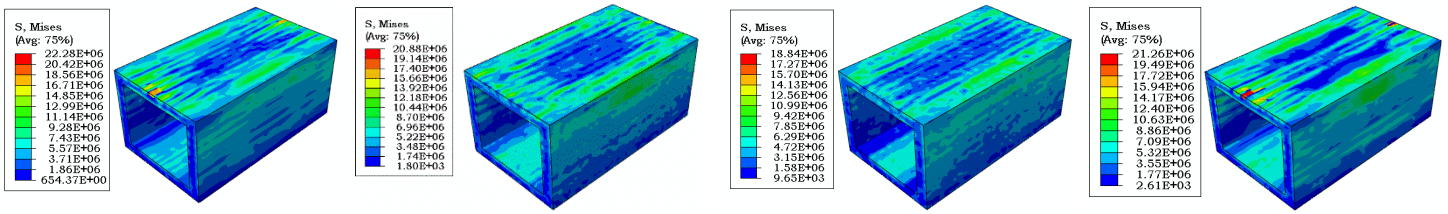

Fig. 7: Contours of the mises stresses in the concrete liner against surface blast (1814 kg TNT) (a) d/H=0.8 (b) d/H=0.9 (c) d/H=1.0 (d) d/H=1.1

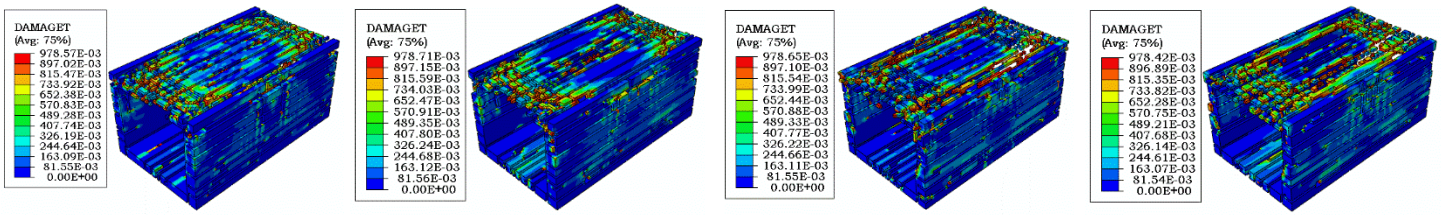

Fig. 8: Tension Damage contours observed in the concrete liner (a) d/H=0.8 (b) d/H=0.9 (c) d/H=1.0 (d) d/H=1.1

5.2. Mitigation Analysis

The description above makes clear how difficult it is to secure the subsurface structure against large blast loads since cut-and-cover tunnels are shallow. Under high-stress circumstances, such as explosions in soft ground, traditional reinforced concrete has shown significant issues. Given this situation, researchers have explored mitigation options, including strengthening the concrete to increase its cut and cover blast resistance or replacing it entirely. It suggests replacing the concrete in tunnel liners with steel fiber-reinforced concrete (SFRC) as a mitigation method, given that concrete is the most commonly used building material against blast loading. It has substituted SFRC for concrete to investigate the impact of an

energy-absorbing material. Mix proportion of SFRC, which contains 2% steel fibers, according to Velasco [18]. The CDP model models this proportion, and Table 5 lists the input parameters [19].

Table 5: Input Properties of the SFRC [19]

Mass Density (kg/m^3)	Young's Modulus (GPa)	Poison's Ratio	Dilation Angle (º)	Eccentricity	f_{b0}/f_{c0}	k	Viscosity Parameter
2521.7	37.673	0.2	24.7	0.1	1.16	0.667	0

The mitigation study has been conducted for the least cover thickness of the soil above the underground structure or cut and cover tunnel. Researchers have reported a 32.72% decrease in mises stresses by replacing the concrete with SFRC. This signifies that SFRC is a better material to reduce the stresses in the tunnel liner. Similarly, the tunnel liner has experienced a significant decrease in settlement values. The use of SFCR instead of concrete resulted in a 96.31% reduction in the maximum settlement in the tunnel liner. This shows that SFRC is a beneficial material for tunnel safety because it absorbs energy. A comparative study was conducted to observe the tensile damage in the tunnel liner following the replacement of the concrete with the new material. Figure 9 indicates a significant reduction in tensile damage. Figure 10 illustrates the comparison of stress, settlement, and tensile damage when utilizing SFRC in place of concrete.

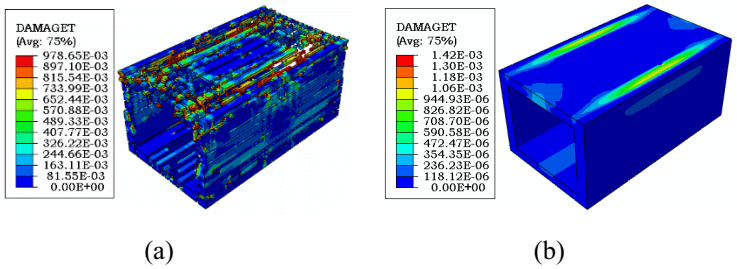

(a) (b)

Fig. 9: Tension Damage (a) Concrete liner (b) SFRC liner

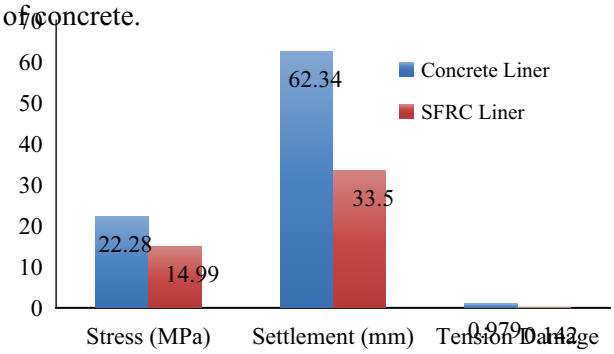

Fig. 10: Compare stress, settlement and tension damage in liner after mitigation

6. Conclusion

The response of an underground tunnel subjected to a surface burst has been analysed in this study. A three-dimensional nonlinear finite element analysis has been carried out in ABAQUS/Explicit. The complete analysis has been segmented in two segments. Effect of Cover Depth and mitigation using SFRC in place of Concrete in tunnel liner

There is the following important conclusion for the present study:

1. The resistance increases against blast load in the concrete tunnel liner by 46.85% when the ratio increases from 0.8 to 1.0, but it decreases by 33.73% when the ratio increases to 1.1. To make the tunnel resistant against the surface blast of a vehicle, soil cover can play a significant role. However, since a cut-and-cover tunnel is shallow by nature, it is reasonable to use it up to a depth of 18 to 20 meters.
2. There have been reports of complete tunnel destruction due to tensile damage. The explosion of the small delivery truck (1814 kg) has caused the liner to collapse catastrophically.
3. One of the foremost conclusions in this study is that an energy-absorbing material, i.e., SFRC, in the present study can play a significant role in improving the resistivity of the cut and cover tunnel against blasts. This study has observed a significant reduction in mises stresses, settlement values, and tensile damage after replacing the concrete with SFRC.

References

[1] Wang, Z., Hao, H., & Lu, Y. (2004). A three-phase soil model for simulating stress wave propagation due to blast loading. International Journal for Numerical and Analytical Methods in Geomechanics, 28(1), 33-56.
[2] Feldgun, V. R., Kochetkov, A. V., Karinski, Y. S., & Yankelevsky, D. Z. (2008). Internal blast loading in a buried lined tunnel. International Journal of Impact Engineering, 35(3), 172-183.
[3] Tiwari, Rohit, Tanusree Chakraborty, and Vasant Matsagar. "Dynamic analysis of tunnel in soil subjected to internal blast loading." *Geotechnical and Geological Engineering* 35 (2017): 1491-1512.
[4] Varma, Malavika, V. B. Maji, and A. Boominathan. "Numerical modeling of a tunnel in jointed rocks subjected to seismic loading." *Underground Space* 4, no. 2 (2019): 133-146.
[5] Goel, M. D., Shivani Verma, Jagriti Mandal, and Sandeep Panchal. "Effect of blast inside tunnel on surrounding soil mass, tunnel lining, and superstructure for varying shapes of tunnels." *Underground Space* 6, no. 6 (2021): 619-635.
[6] Sadique, Md Rehan, Mohammad Zaid, and Mohd Masroor Alam. "Rock tunnel performance under blast loading through finite element analysis." *Geotechnical and Geological Engineering* 40, no. 1 (2022): 35-56.
[7] Kasilingam, Senthil, Muskaan Sethi, Loizos Pelecanos, and Narinder K. Gupta. "Mitigation strategies of underground tunnels against blast loading." International Journal of Protective Structures 13, no. 1 (2022): 21-44.
[8] Abaqus, G. "Abaqus 6.11." Dassault Systemes Simulia Corporation, Providence, RI, USA (2011): 3.
[9] Bhowmik, D., D. K. Baidya, and S. P. Dasgupta. "A numerical and experimental study of hollow steel pile in layered soil subjected to vertical dynamic loading." *Soil dynamics and earthquake engineering* 85 (2016): 161-165.
[10] Sadique, M. R., Mohammad Ashraf Iqbal, and Pradeep Bhargava. "Nuclear containment structure subjected to commercial and fighter aircraft crash." *Nuclear Engineering and Design* 260 (2013): 30-46.
[11] Hafezolghorani, Milad, Farzad Hejazi, Ramin Vaghei, Mohd Saleh Bin Jaafar, and Keyhan Karimzade. "Simplified damage plasticity model for concrete." *Structural engineering international* 27, no. 1 (2017): 68-78.
[12] Johnson, G. R. (1983). A constitutive model and data for materials subjected to large strains, high strain rates, and high temperatures. Proc. 7th Inf. Sympo. Ballistics, 541-547.
[13] Goel, M. D., Matsagar, V. A., & Gupta, A. K. (2011). Dynamic response of stiffened plates under air blast. International Journal of Protective Structures, 2(1), 139-155.
[14] Mussa, Mohamed H., Azrul A. Mutalib, Roszilah Hamid, Sudharshan R. Naidu, Noor Azim Mohd Radzi, and Masoud Abedini. "Assessment of damage to an underground box tunnel by a surface explosion." *Tunnelling and underground space technology* 66 (2017): 64-76
[15] Kingery, Charles N., Gerald Bulmash, Peter Muller, and ARMY BALLISTIC RESEARCH LAB ABERDEEN PROVING GROUND MD. *Blast Loading on Above-ground Barricaded Munition Storage Magazines*. Ballistic Research Laboratories, 1984.
[16] Shukla, Palak J., Atul K. Desai, and Chetankumar D. Modhera. "Dynamic response of cut and cover tunnel section under blast loading." *Innovative Infrastructure Solutions* 6 (2021): 1-23.
[17] Ambrosini, Ricardo Daniel, and Bibiana María Luccioni. "Craters produced by explosions on the soil surface." *Journal of applied mechanics* 73, no. 6 (2006): 890-900.
[18] Velasco, R. V. "Self-consolidating concretes reinforced with high volumetrics fractions of steel fibers: Rheological, physics, mechanics and thermal properties." *PhD diss., Ph. D. Thesis. COPPE, Federal University of Rio de Janeiro, Rio de Janeiro* (2008).
[19] An, Chen, Xavier Castello, Menglan Duan, Romildo D. Toledo Filho, and Segen F. Estefen. "Ultimate strength behaviour of sandwich pipes filled with steel fiber reinforced concrete." *Ocean Engineering* 55 (2012): 125-135.